Supplemental Information for:

Fluorescent biological aerosol particle concentrations and size distributions measured with an ultraviolet aerodynamic particle sizer (UV-APS) in central Europe

J. A. Huffman[1], B. Treutlein[1,2], and U. Pöschl[1*]

[1]*Max Planck Institute for Chemistry, Biogeochemistry Department, Becherweg 27, D-55128 Mainz, Germany*
[2]*Now at Ludwig Maximilians University, Institute for Physical Chemistry, Munich, Germany*

[*]*Corresponding author: poeschl@mpch-mainz.mpg.de, +49 (6131) 305 422*

Major Version 8
Submitted to ACPD publication August 7, 2009

Supplemental Table and Figure Captions

Table S1: UV-APS instrument statistics shown for each of 52 particle size channels. $D_{a,g}$ shows geometric median value of the upper and lower range for aerodynamic particle diameter . $D_{a,low}$ refers to the lower particle size bound. Lowest detectable concentration (LDC) as absolute value (dM) and normalized to width of size bin (dM/dlogD_a). Campaign mean values of d$N_{T,c}$, d$N_{T,c,}$ d$N_{F,c,}$ d$M_{T,c,}$ d$M_{F,c}$ shown per size bin.

Figure S1: Example of standard particle size calibration curve for UV-APS. Aerodynamic diameter (D_a) measured by UV-APS plotted vs. D_a of polystyrene latex spheres (PSL) of varying diameter. Data points show nebulized PSLs, and black trace is a linear fit to the data. Physical diameter (D_p) of PSLs were converted to D_a using a density, $\rho = 1.05$ g/cm^3 and dynamic shape factor, $X = 1.0$. Linear fit of data has equation: y = 1.028x + 0.0043.

Figure S2: Time series of FBAP number concentrations for the entire measurement period using fluorescence bins ≥ 2 (to compare with "standard" analysis using bins ≥ 3). **(a)** Integrated $N_{F2,c}$ on left axis (green) and FBAP fraction of TAP number ($N_{F2,c}$ / $N_{T,c}$) on right axis (black). **(b)** Image plot of FBAP number with aerodynamic diameter shown logarithmically on y-axis and date on x-axis. Color scale shows dN_{F2}/dlogD_a. Details are analogous to Figure 12.

Figure S3: Time series of FBAP number concentration factor increase using fluorescence bins ≥ 2 compared with using fluorescence bins ≥ 3. **(a)** Ratio of integrated $N_{F2,c}$ / $N_{F,c}$. **(b)** Image plot of ratio between d$N_{F2,c}$ and d$N_{F,c}$ with aerodynamic diameter shown logarithmically on y-axis and date on x-axis. Color scale shows factor increase in $N_{F2,c,}$ with white values shown at an arbitrary point for visual clarity.

Figure S4: Size distribution of factor increase in of integrated d$N_{F2,c}$ compared to d$N_{F,c}$. Campaign-mean size distribution for d$N_{F2,c}$/dlogD_a for fluorescence bins ≥ 2 divided by dN_F,c/dlogD_a for fluorescence bins ≥ 3.

Figure S5: Scatter plots of N_F vs. N_T for particle diameters below **(a)** and above **(b)** 1.0 μm, respectively. $D_a \leq 0.965$ μm and $D_a \geq 1.037$ μm geometric mid-point of UV-APS size channels 9 and 10, respectively. $N_{F,<0.965}$ particle number exhibiting fluorescence in the fine particle mode (< 1.0 μm) and $N_{T,<0.965}$ all particles in size mode. $N_{F,>1.037}$ and $N_{T,>1.037}$, coarse mode (> 1.0 μm). Data points are colored by date of measurement; note that later points obscure earlier points. Black lines are linear fits to all data in each plot, with equations and Pearson's R-squared values as follows: (a) y = 0.000918x + 0.000786, $R^2 = 0.51$, (b) y = 0.0102x + 0.0178, $R^2 = 0.17$.

Figures S6: Scatter plots of N_F vs. N_T for particle diameters below **(a)** and above **(b)** 0.75 μm, respectively. Details are analogous to Figure S5, except that $D_a \leq 0.723$ μm and $D_a \geq 0.777$ μm geometric mid-point of UV-APS size channels 5 and 6, respectively. (a) y = 0.000867x + 0.000150, $R^2 = 0.87$, (b) y = 0.00221x + 0.0224, $R^2 = 0.11$.

Figure S7: Time series of TAP number concentrations and size distributions for the entire measurement period (3 August – 4 December 2006). **(a)** Integrated coarse TAP concentration (1-20 μm, $N_{T,c}$) on left axis (green) and FBAP fraction of TAP number ($N_{F,c}$ / $N_{T,c}$) on right axis (black). Note that axes are logarithmically scaled and off-set from one another. Each data point represents a five-minute measurement. **(b)** TAP size distribution with date on x-axis, aerodynamic diameter on y-axis, and color scale of dN_T/dlogD_a with white values set to $LDC_{dN/dlogDa} = 6.4 \times 10^{-3}$ cm^{-3}. Dashed black line at 1.0 μm shows particle size cut-off below which fluorescent particles were not considered FBAP due to interference with non-biological aerosol.

Figure S8: Time series of TAP number concentrations (panel top halves) and size distributions (panel bottom halves) for each month of the measurement period (plots analogous to Fig. S7): **(a)** August, **(b)** September, **(c)** October, and **(d)** November (extending to December 4).

Figure S9: Diel cycles of TAP number concentrations and size distributions for the entire measurement period (hourly median values vs. local time of day). **(a)** Integrated coarse TAP concentration (1-20 μm, $N_{T,c}$) on left axis (green) and FBAP fraction of TAP number ($N_{F,c}$ / $N_{T,c}$) on right axis (black). **(b)** TAP size distribution with hour of day on x-axis, aerodynamic diameter on y-axis and color scale of $dN_T/d\log D_a$ with white values set to 0.5 cm^{-3} for visual clarity. Dashed black line at 1.0 μm shows particle size cut-off below which fluorescent particles were not considered FBAP due to interference with non-biological aerosol.

Figure S10: Diel cycles of TAP number concentrations (panel top halves) and size distributions (panel bottom halves) for each month of the measurement period (plots analogous to Fig. S9): **(a)** August, **(b)** September, **(c)** October, and **(d)** November.

Figure S11: Diel cycles of FBAP mass concentrations (panel top halves) and size distributions (panel bottom halves) for each month of the measurement period (plots analogous to Fig. S9): **(a)** August, **(b)** September, **(c)** October, and **(d)** November.

Figure S12: Time series of TAP mass concentrations and size distributions for the entire measurement period (3 August – 4 December 2006). **(a)** Integrated coarse TAP concentration (1-20 μm, $M_{T,c}$) on left axis (green) and FBAP fraction of TAP mass ($M_{F,c}$ / $M_{T,c}$) on right axis (black). Note that axes are logarithmically scaled and off-set from one another. Each data point represents a five-minute measurement. **(b)** TAP size distribution with date on x-axis, aerodynamic diameter on y-axis, and color scale of $dN_T/d\log D_a$ with white values set to 6.4×10^{-3} μg m^{-3} for visual clarity. Dashed black line at 1.0 μm shows particle size cut-off below which fluorescent particles were not considered FBAP due to interference with non-biological aerosol.

Figure S13: Time series of TAP number concentrations (panel top halves) and size distributions (panel bottom halves) for each month of the measurement period (plots analogous to Fig. S12): **(a)** August, **(b)** September, **(c)** October, and **(d)** November (extending to December 4).

Figure S14: Diel cycles of FBAP mass concentrations (panel top halves) and size distributions (panel bottom halves) for each month of the measurement period (plots analogous to Fig. 8): **(a)** August, **(b)** September, **(c)** October, and **(d)** November.

Figure S15: Normalized FBAP number concentration, $dN_F/d\log D_a$ for exemplary period #1 (Fig. 9a – b).

Figure S16: Characteristic FBAP number size distribution patterns observed during exemplary periods #7 and #8. Left panels show time series of $N_{F,c}$, $N_{F,c}$ / $N_{T,c}$ ratio and $dN_F/d\log D_a$ on days of interest (analogous to Fig. 1), and black vertical lines indicate time periods over which exemplary size distributions were averaged ($dN_F/d\log D_a$ vs D_a, right panels). Red traces represent mean values, green traces represent median values, dark gray regions show 25 – 75th percentile range, and light gray regions show 5 – 95th percentile range. Hatched area below 1.0 μm indicates particle size range where fluorescent particles were not considered FBAP due to interference with non-biological aerosol. **(a–b)** Period #7: 7 September 05:46 – 07:26, **(c-d)** Period #8: 26 October 05:54 – 10:34.

Figure S17: Characteristic FBAP number size distribution patterns observed during exemplary periods #9 and #10 (plots analogous to Fig. S16). **(a-b)** Period #9: 15 August 00:08 – 04:48, **(c–d)** Period #10: 19 August 22:59 – 20 August 06:39.

Figure S18: Characteristic FBAP number size distribution patterns observed during exemplary periods #11 and #12 (plots analogous to Fig. S16). **(a-b)** Period #11: 30 September 12:24 – 19:34, **(c–d)** Period #12: 10 September 04:57 – 11 September 03:32.

Figure S19: Average TAP number size distributions for each month of the measurement period. Red traces represent mean values, green traces represent median values, dark gray regions show 25 – 75th percentile range, and light gray regions show 5 – 95th percentile range. Hatched area below 1.0 μm indicates particle size range where fluorescent particles were not considered FBAP due to interference with non-biological aerosol. **(a)** August, **(b)** September, **(c)** October, **(d)** November.

Figure S20: Campaign average TAP number size distribution. Reproduced from Figure 12a, replacing y-axis with logarithmic scale.

Figure S21: Average TAP mass size distributions for each month of the measurement period (plots analogous to Fig. S19). **(a)** August, **(b)** September, **(c)** October, **(d)** November.

Figure S22: Average FBAP mass size distributions for each month of the measurement period (plots analogous to Fig. S19). **(a)** August, **(b)** September, **(c)** October, **(d)** November.

Figure S23: Average size distribution of the FBAP to TAP number concentration ratio (d$N_{F,c}$ / d$N_{T,c}$) for the entire measurement period (plot analogous to Fig. S19). **(a)** August, **(b)** September, **(c)** October, **(d)** November.

Figure S24: Average size distribution of the FBAP to TAP number concentration ratio (d$N_{F,c}$ / d$N_{T,c}$) for the entire measurement period after removing period from 10 – 29 October (plot analogous to Fig. S19).

Channel #	$D_{a,g}$ (μm)	$D_{a,low}$ (μm)	LDC dM (μg m^{-3})	LDC dM/dlogD_a (μg m^{-3})	Campaign Mean Values			
					d$N_{T,c}$ (cm^{-3})	d$N_{F,c}$ (cm^{-3})	d$M_{T,c}$ (μg m^{-3})	d$M_{F,c}$ (μg m^{-3})
1	0.300	-	0.000003	0.000011	0.420	0.00038	0.0059	0.00001
2	0.542	0.523	0.000017	0.000534	0.329	0.00030	0.0274	0.00003
3	0.583	0.562	0.000021	0.000664	0.499	0.00046	0.0518	0.00005
4	0.626	0.604	0.000026	0.000822	0.644	0.00059	0.0828	0.00008
5	0.673	0.649	0.000032	0.00102	0.844	0.00078	0.135	0.00012
6	0.723	0.697	0.000040	0.00127	0.940	0.00089	0.186	0.00018
7	0.777	0.749	0.000049	0.00157	0.949	0.00094	0.233	0.00023
8	0.835	0.805	0.000061	0.00195	0.767	0.00083	0.234	0.00025
9	0.898	0.865	0.000076	0.00243	0.536	0.00067	0.203	0.00025
10	0.965	0.930	0.000094	0.00301	0.367	0.00057	0.173	0.00027
11	1.037	0.999	0.000117	0.00374	0.256	0.00054	0.149	0.00032
12	1.114	1.074	0.000145	0.00463	0.162	0.00048	0.117	0.00035
13	1.197	1.154	0.000180	0.00575	0.120	0.00049	0.108	0.00044
14	1.286	1.240	0.000223	0.00713	0.101	0.00055	0.113	0.00062
15	1.382	1.333	0.000276	0.00885	0.0808	0.00056	0.112	0.00077
16	1.486	1.432	0.000344	0.0110	0.0707	0.00059	0.122	0.00102
17	1.596	1.539	0.000426	0.0136	0.0614	0.00061	0.131	0.00131
18	1.715	1.654	0.000528	0.0169	0.0487	0.00060	0.129	0.00160
19	1.843	1.777	0.000656	0.0210	0.0445	0.00069	0.146	0.00225
20	1.981	1.910	0.000814	0.0261	0.0376	0.00078	0.153	0.00316
21	2.129	2.052	0.00101	0.0323	0.0307	0.00087	0.155	0.00438
22	2.288	2.205	0.00125	0.0401	0.0294	0.00118	0.185	0.0073863
23	2.458	2.370	0.00156	0.0498	0.0238	0.00136	0.185	0.0106
24	2.642	2.547	0.00193	0.0618	0.0214	0.00166	0.206	0.0160
25	2.839	2.737	0.00240	0.0767	0.0182	0.00182	0.218	0.0218
26	3.051	2.941	0.00297	0.0952	0.0159	0.00195	0.237	0.0290
27	3.278	3.160	0.00369	0.118	0.0131	0.00190	0.242	0.0351
28	3.523	3.396	0.00458	0.147	0.0108	0.00180	0.246	0.0413
29	3.786	3.650	0.00568	0.182	0.00866	0.00160	0.246	0.0454
30	4.068	3.922	0.00705	0.226	0.00691	0.00138	0.244	0.0488
31	4.371	4.215	0.00875	0.280	0.00549	0.00117	0.240	0.0510
32	4.698	4.529	0.0109	0.347	0.00430	0.00096	0.234	0.0519
33	5.048	4.867	0.0135	0.431	0.00320	0.00073	0.216	0.0493
34	5.425	5.230	0.0167	0.535	0.00242	0.00057	0.203	0.0479
35	5.829	5.620	0.0207	0.664	0.00187	0.00045	0.193	0.0463
36	6.264	6.040	0.0257	0.824	0.00157	0.00039	0.202	0.0499
37	6.732	6.490	0.0319	1.02	0.00122	0.00032	0.195	0.0517
38	7.234	6.974	0.0396	1.27	0.00102	0.00029	0.202	0.0572
39	7.774	7.495	0.0492	1.57	0.00079	0.00024	0.195	0.0588
40	8.354	8.054	0.0611	1.95	0.00061	0.00019	0.185	0.0585
41	8.977	8.655	0.0758	2.42	0.00045	0.00014	0.169	0.0544
42	9.647	9.300	0.0940	3.01	0.00033	0.00011	0.157	0.0499
43	10.370	9.994	0.117	3.74	0.00024	0.00008	0.141	0.0449
44	11.140	10.740	0.145	4.63	0.00018	0.00005	0.128	0.0391
45	11.970	11.541	0.180	5.75	0.00014	0.00004	0.124	0.0381
46	12.860	12.402	0.223	7.13	0.00013	0.00006	0.145	0.0619
47	13.820	13.328	0.276	8.85	0.00011	0.00004	0.146	0.0577
48	14.860	14.322	0.344	11.00	0.00010	0.00003	0.166	0.0595
49	15.960	15.390	0.426	13.62	0.00008	0.00002	0.168	0.0354
50	17.150	16.539	0.528	16.90	0.00007	0.00001	0.182	0.01546
51	18.430	17.773	0.656	20.98	0.00007	0.000002	0.214	0.00759
52	19.810	19.099	0.814	26.05	0.00006	0.000001	0.258	0.00526

Table S1.

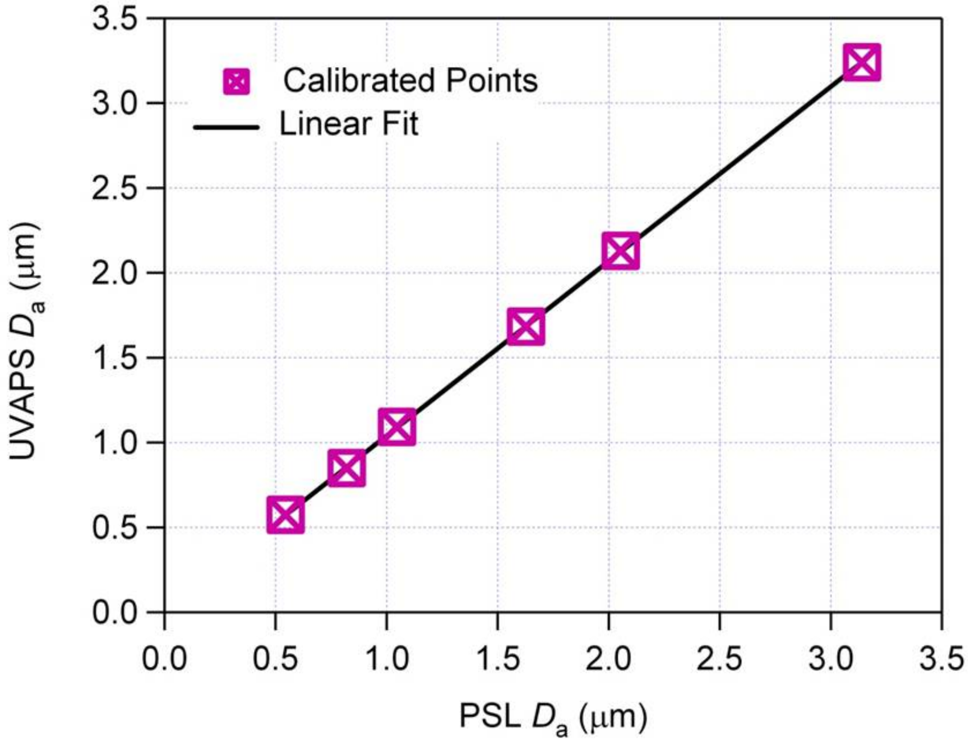
Calibrated Points
Linear Fit
UVAPS D_a (μm)
PSL D_a (μm)
0.0
0.5
1.0
1.5
2.0
2.5
3.0
3.5

Figure S1.

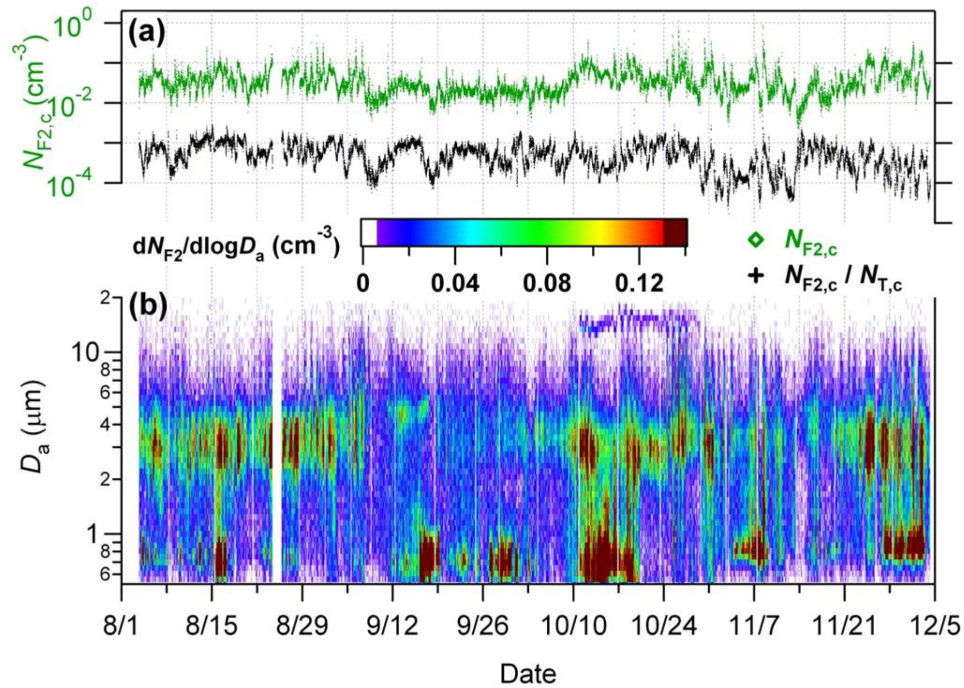
(a)
N_F2,c (cm^-3)
10^0
10^-2
10^-4
10^1
10^-1
10^-3
N_F2,c / N_T,c
dN_F2/dlogD_a (cm^-3)
0
0.04
0.08
0.12
N_F2,c
N_F2,c / N_T,c
(b)
D_a (µm)
2
10
8
6
4
2
1
8
6
8/1
8/15
8/29
9/12
9/26
10/10
10/24
11/7
11/21
12/5
Date

Figure S2.

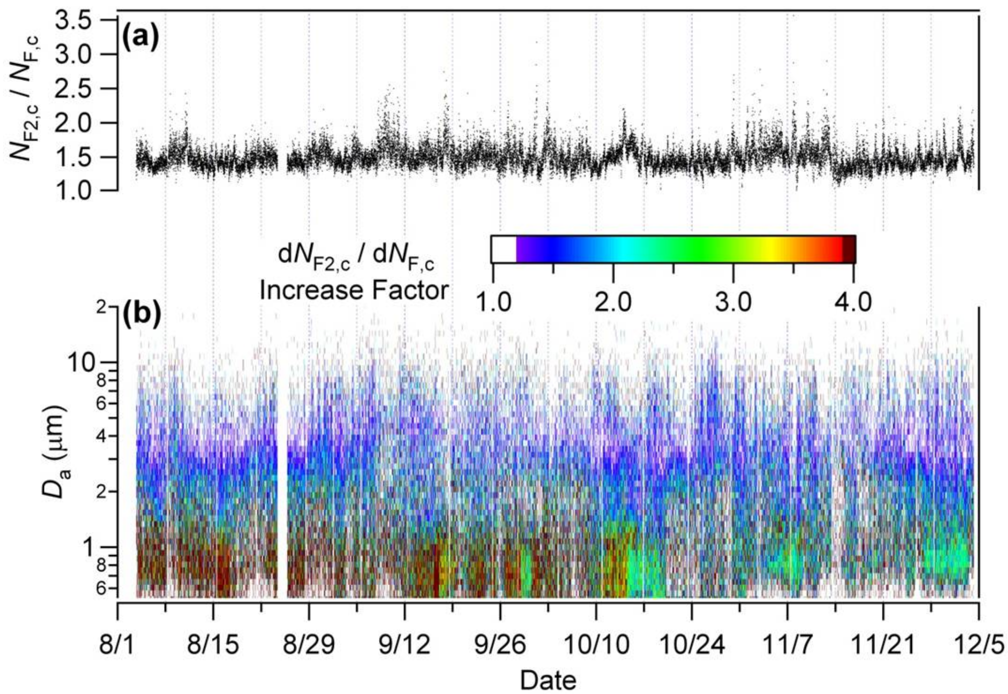
(a)
N F2,c / N F,c
3.5
3.0
2.5
2.0
1.5
1.0
dN F2,c / dN F,c
Increase Factor
1.0
2.0
3.0
4.0
(b)
D a (µm)
2
10
8
6
4
2
1
8
6
8/1
8/15
8/29
9/12
9/26
10/10
10/24
11/7
11/21
12/5
Date

Figure S3.

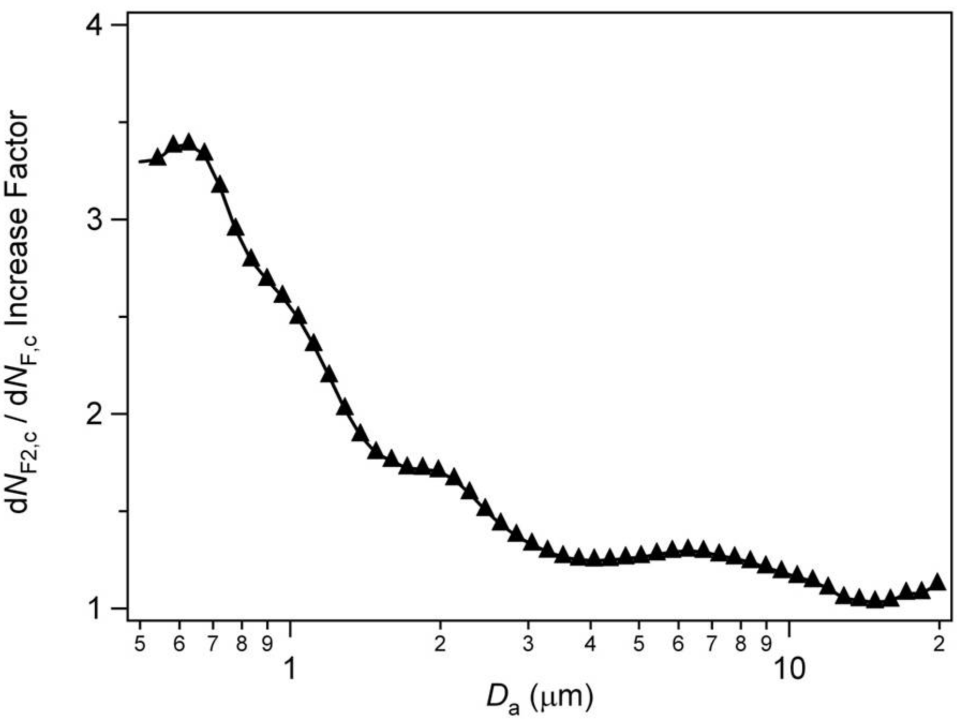

Figure S4.

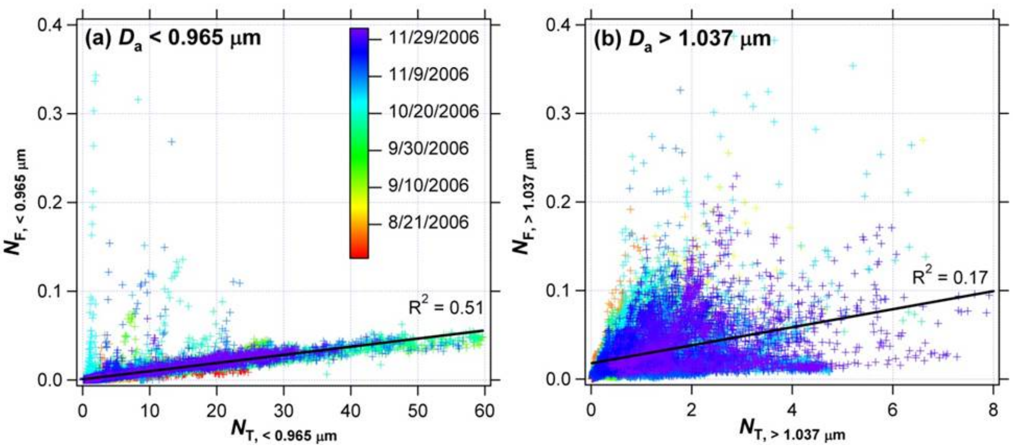
(a) D_a < 0.965 µm
11/29/2006
11/9/2006
10/20/2006
9/30/2006
9/10/2006
8/21/2006
R^2 = 0.51
$N_{F, < 0.965\ µm}$
$N_{T, < 0.965\ µm}$
0.0
0.1
0.2
0.3
0.4
0
10
20
30
40
50
60
(b) D_a > 1.037 µm
R^2 = 0.17
$N_{F, > 1.037\ µm}$
$N_{T, > 1.037\ µm}$
0.0
0.1
0.2
0.3
0.4
0
2
4
6
8

Figure S5.

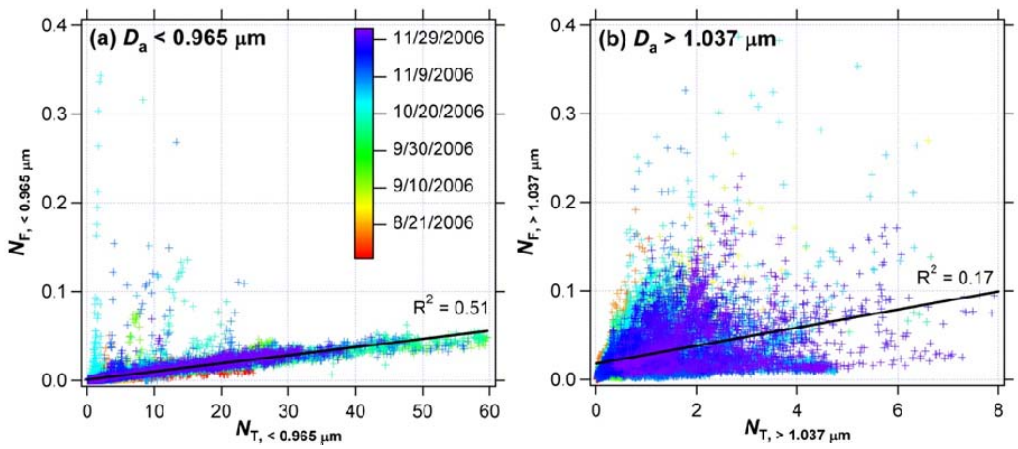
(a) D_a < 0.965 µm
11/29/2006
11/9/2006
10/20/2006
9/30/2006
9/10/2006
8/21/2006
R^2 = 0.51
$N_{F, < 0.965\ \mu m}$
$N_{T, < 0.965\ \mu m}$
(b) D_a > 1.037 µm
R^2 = 0.17
$N_{F, > 1.037\ \mu m}$
$N_{T, > 1.037\ \mu m}$

Figure S6.

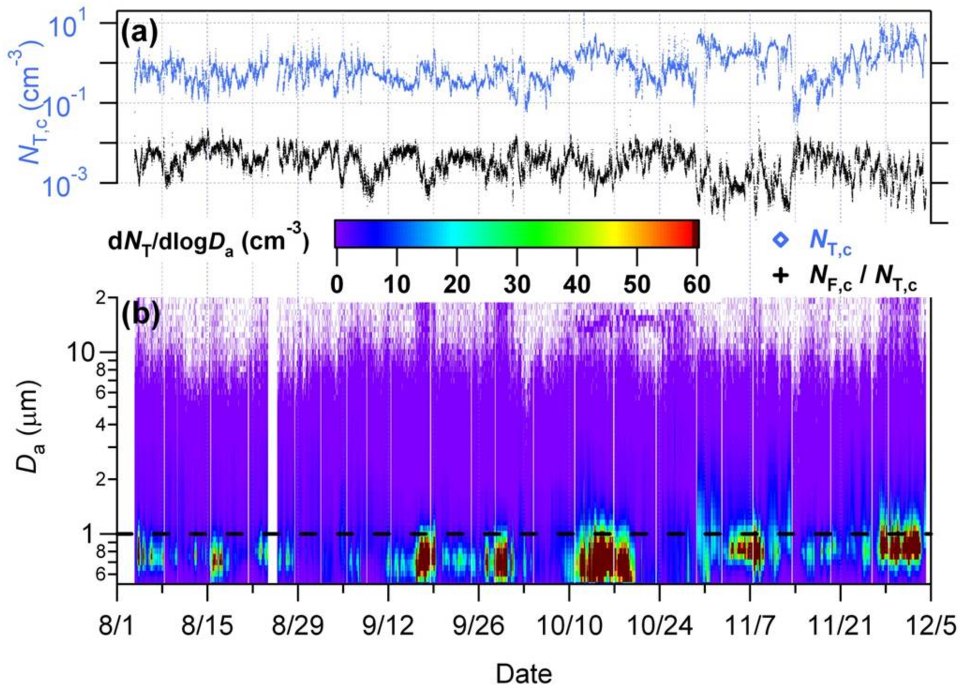
(a)
$N_{T,c}$ (cm^{-3})
10^1
10^{-1}
10^{-3}
$N_{F,c}$ / $N_{T,c}$ (%)
10^3
10^1
10^{-1}
dN_T/dlogD_a (cm^{-3})
0 10 20 30 40 50 60
$N_{T,c}$
$N_{F,c}$ / $N_{T,c}$
(b)
D_a (μm)
8/1 8/15 8/29 9/12 9/26 10/10 10/24 11/7 11/21 12/5
Date

Figure S7.

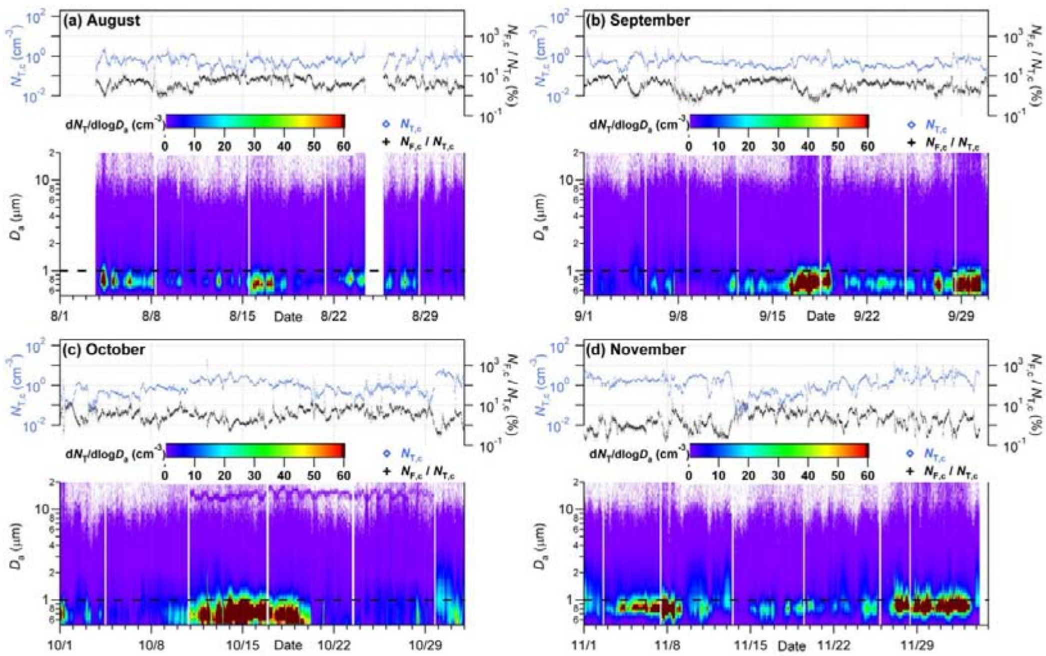
(a) August
(b) September
(c) October
(d) November
Date
dN_T/dlogD_a (cm^-3)
N_T,c
N_F,c / N_T,c
D_a (μm)

Figure S8.

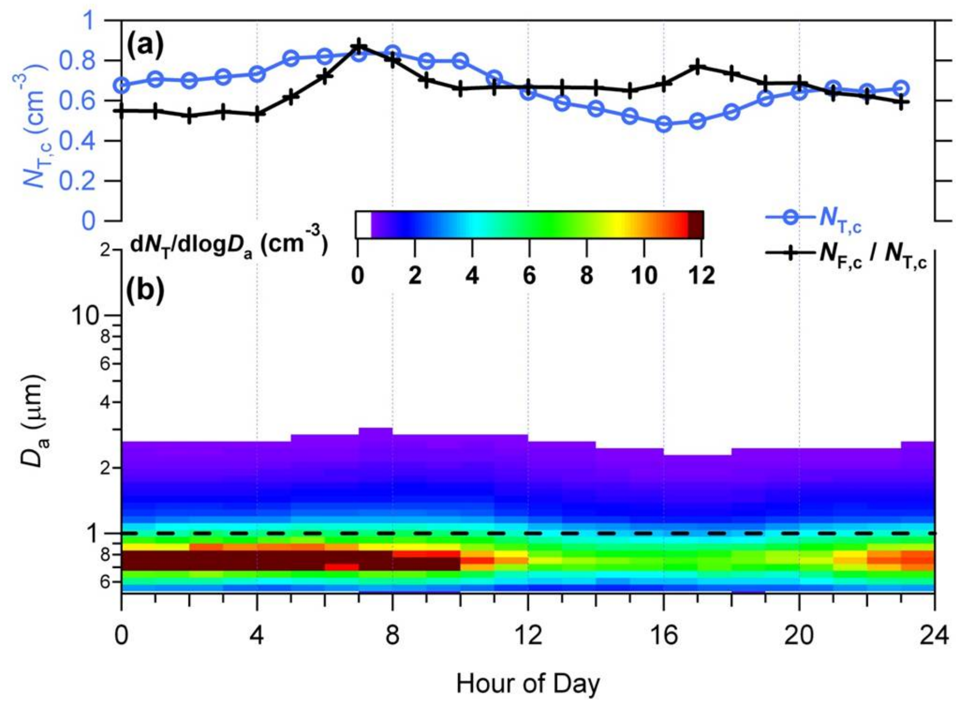
(a)
(b)
$N_{T,c}$ (cm^{-3})
$N_{F,c}$ / $N_{T,c}$ (%)
$N_{T,c}$
$N_{F,c}$ / $N_{T,c}$
dN_T/dlogD_a (cm^{-3})
0 2 4 6 8 10 12
D_a (µm)
Hour of Day

Figure S9.

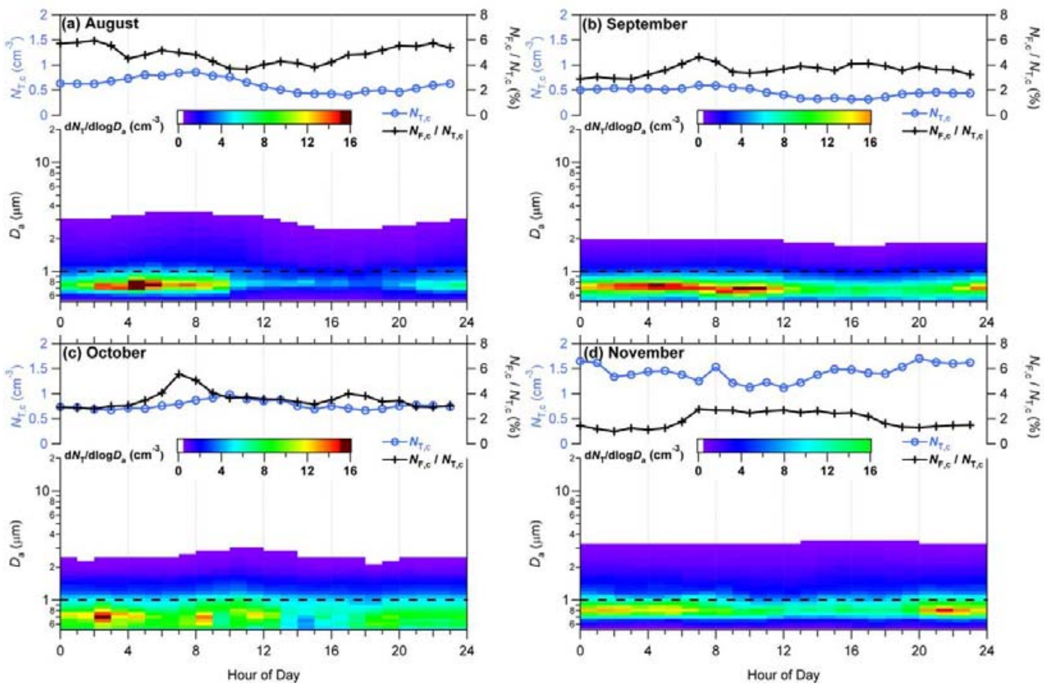

Figure S10.

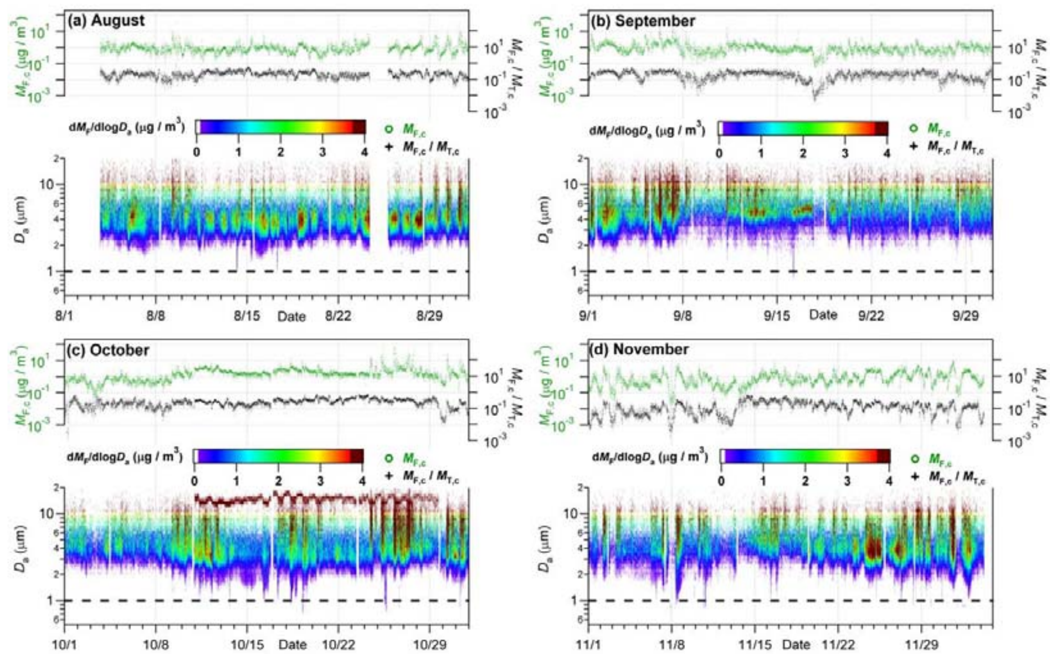
(a) August
(b) September
(c) October
(d) November
$dM_F/d\log D_a$ (µg / m³)
$M_{F,c}$
$M_{F,c}$ / $M_{T,c}$
$M_{F,c}$ (µg / m³)
D_a (µm)
Date
8/1
8/8
8/15
8/22
8/29
9/1
9/8
9/15
9/22
9/29
10/1
10/8
10/15
10/22
10/29
11/1
11/8
11/15
11/22
11/29

Figure S11.

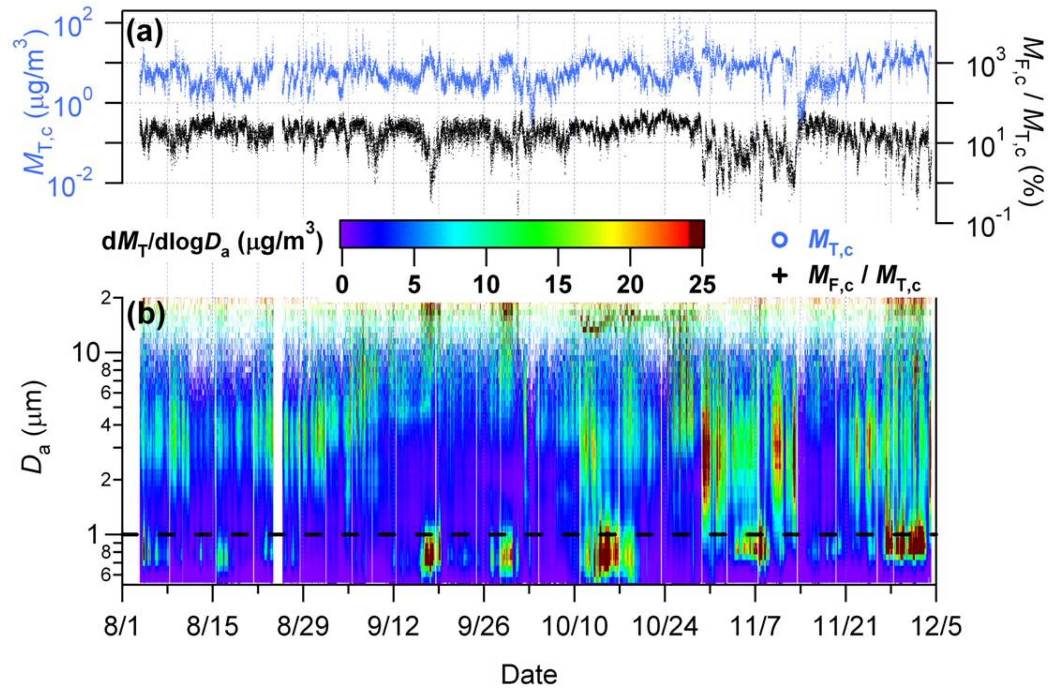

Figure S12.

8/7/2009

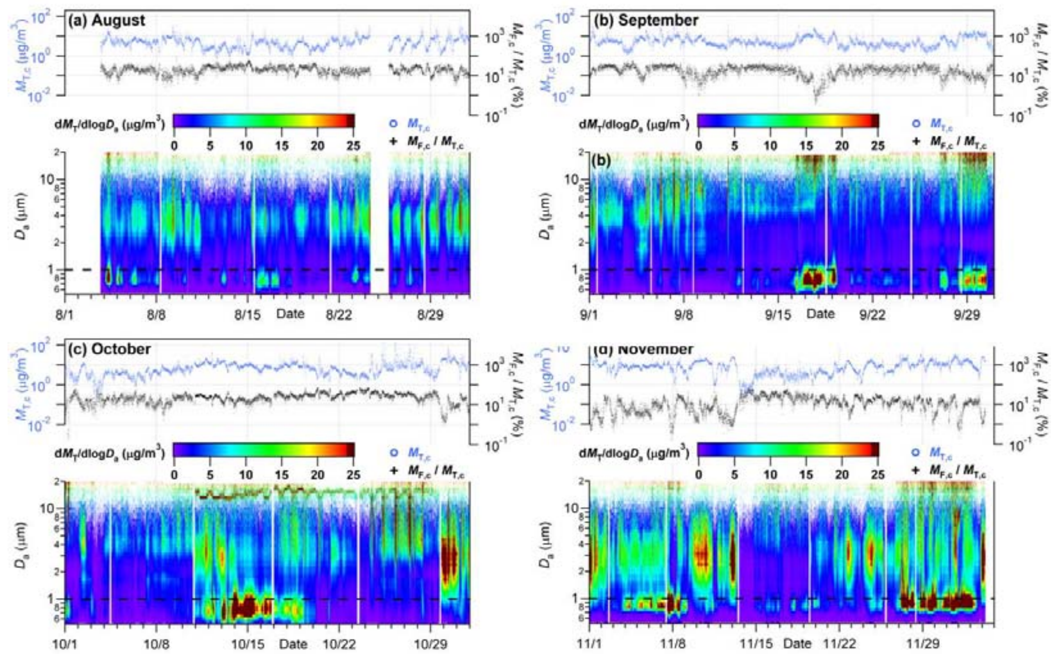
(a) August
(b) September
(c) October
(d) November
dM_T/dlogD_a (µg/m³)
0 5 10 15 20 25
M_T,c
M_F,c / M_T,c
M_T,c (µg/m³)
M_F,c / M_T,c (%)
D_a (µm)
Date
8/1 8/8 8/15 8/22 8/29
9/1 9/8 9/15 9/22 9/29
10/1 10/8 10/15 10/22 10/29
11/1 11/8 11/15 11/22 11/29

Figure S13.

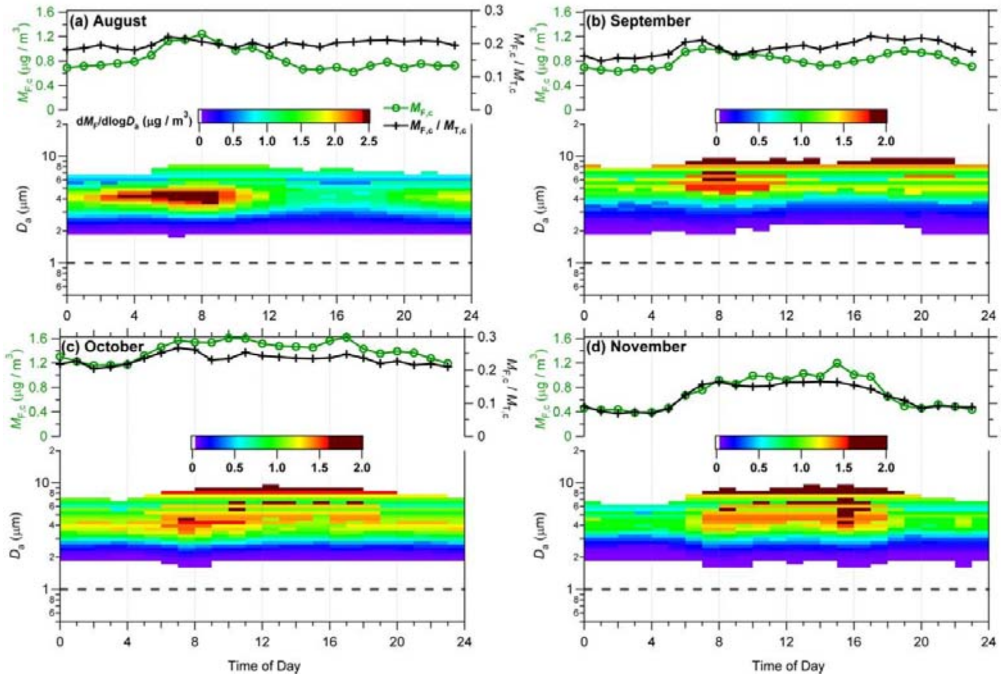
(a) August
(b) September
(c) October
(d) November
$M_{F,c}$ (µg / m³)
$M_{F,c}$ / $M_{T,c}$
dMF/dlogDa (µg / m³)
D_a (µm)
Time of Day

Figure S14.

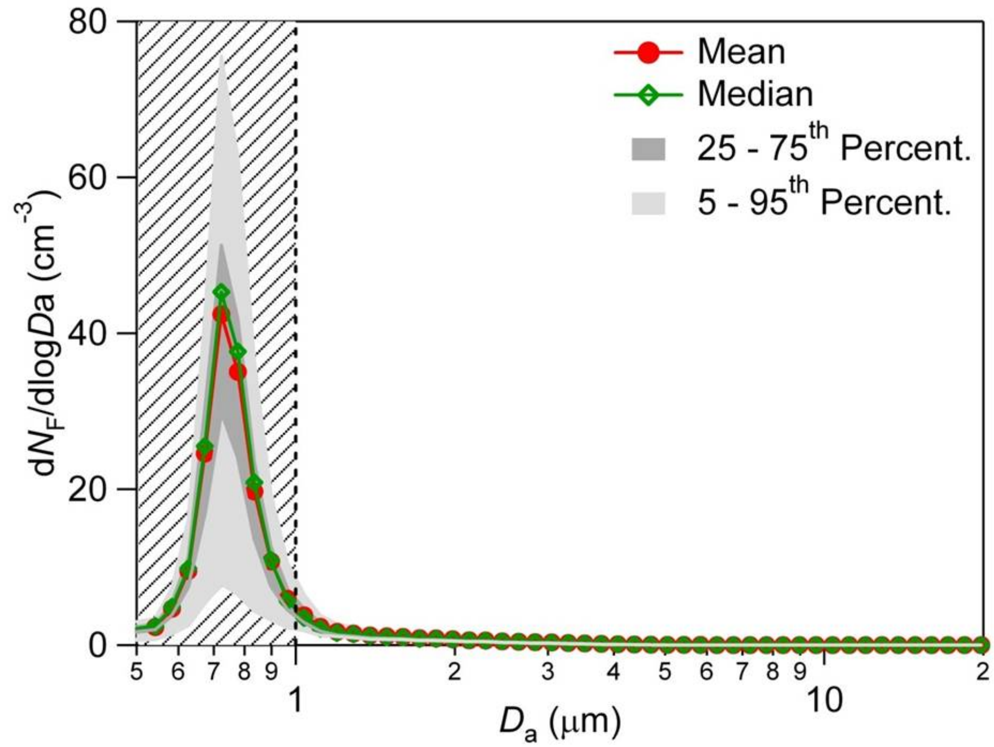
80
60
40
20
0
dN_F/dlogDa (cm^-3)
Mean
Median
25 - 75th Percent.
5 - 95th Percent.
5 6 7 8 9
1
2
3
4
5 6 7 8 9
10
2
D_a (μm)

Figure S15.

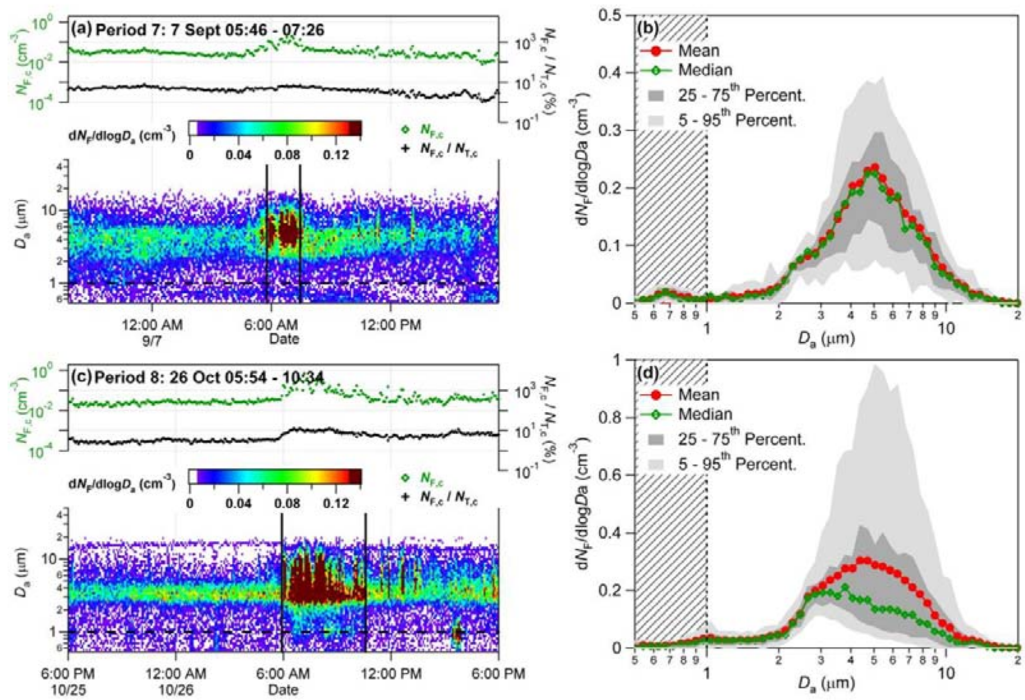
(a) Period 7: 7 Sept 05:46 - 07:26
(b)
(c) Period 8: 26 Oct 05:54 - 10:34
(d)
Mean
Median
25 - 75th Percent.
5 - 95th Percent.
dNF/dlogDa (cm-3)
Da (µm)
Date
12:00 AM 9/7
6:00 AM
12:00 PM
6:00 PM 10/25
12:00 AM 10/26
6:00 PM

Figure S16.

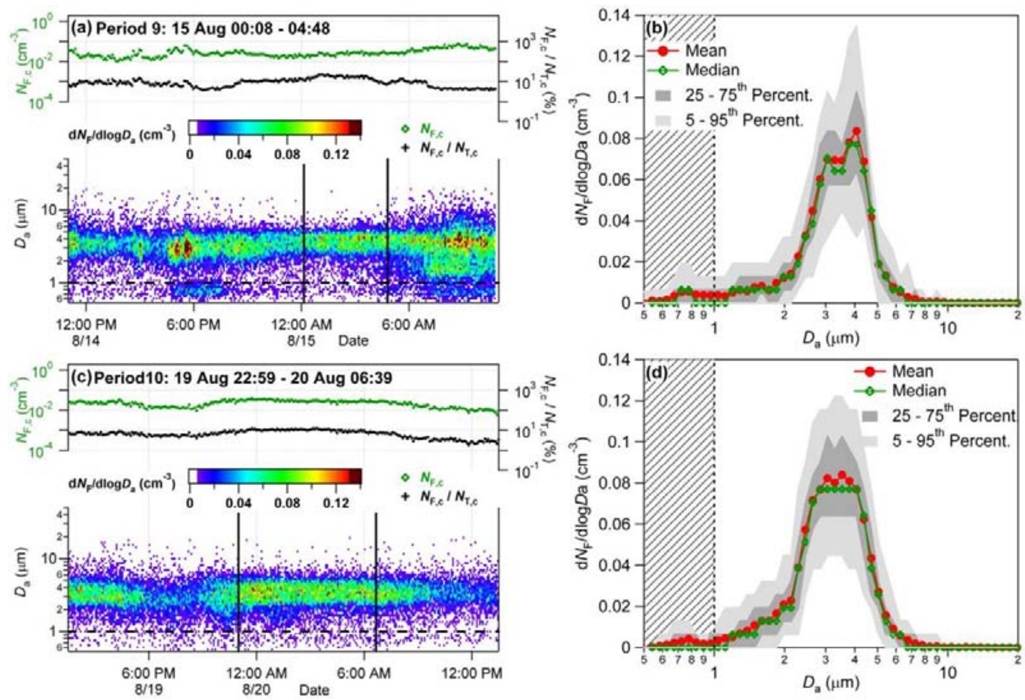

202

203 **Figure S17.**

204

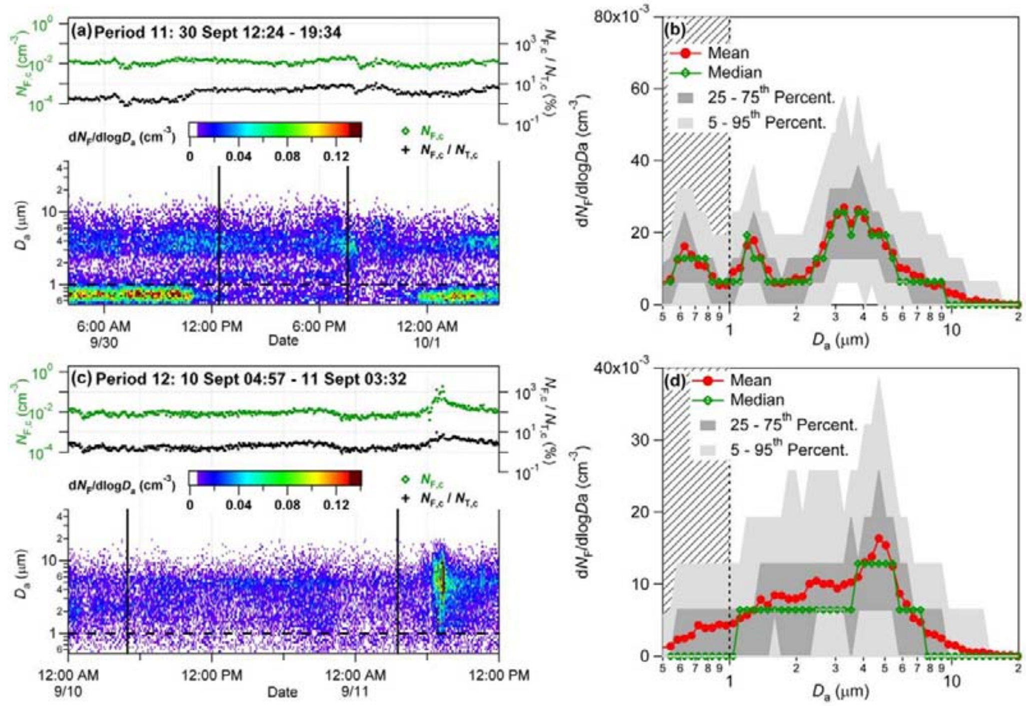
(a) Period 11: 30 Sept 12:24 - 19:34
(b)
Mean
Median
25 - 75th Percent.
5 - 95th Percent.
(c) Period 12: 10 Sept 04:57 - 11 Sept 03:32
(d)
dNF/dlogDa (cm-3)
Da (μm)
Date
6:00 AM 9/30
12:00 PM
6:00 PM
12:00 AM 10/1
12:00 AM 9/10
12:00 AM 9/11
0.04
0.08
0.12

Figure S18.

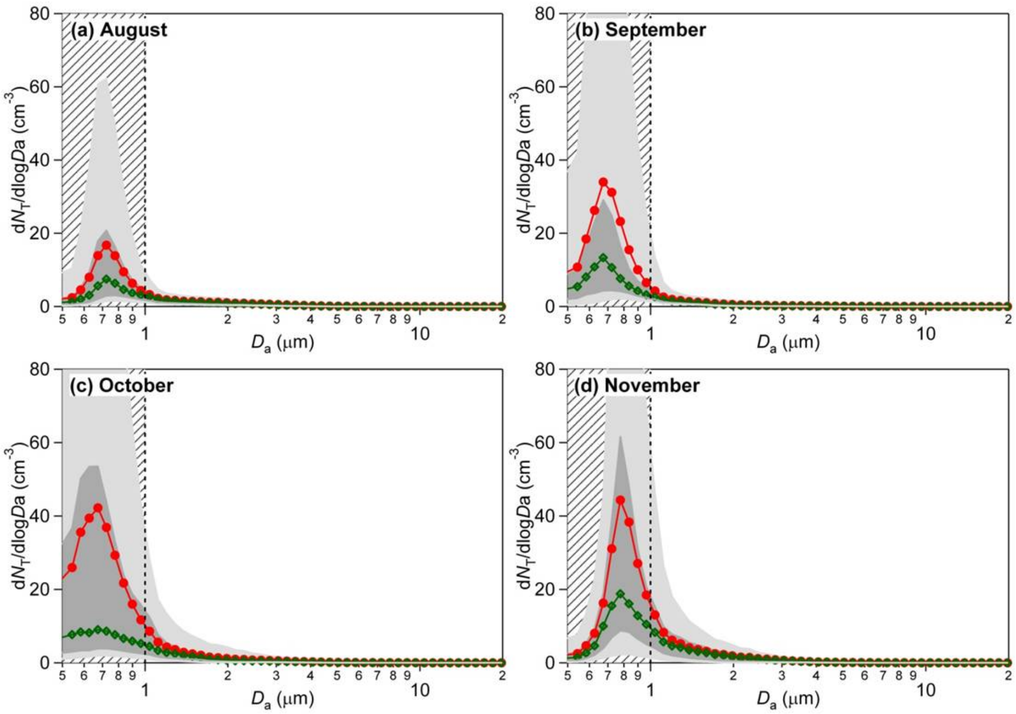
(a) August
(b) September
(c) October
(d) November
dN_T/dlogDa (cm^-3)
D_a (μm)
0
20
40
60
80
5 6 7 8 9 1 2 3 4 5 6 7 8 9 10 2

Figure S19.

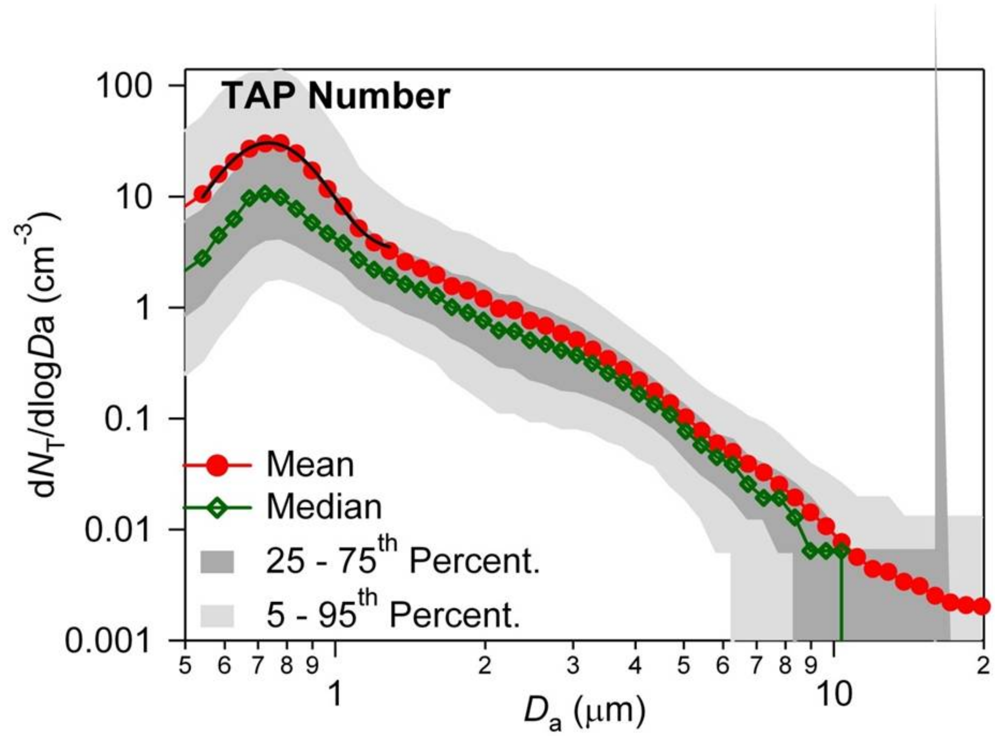
TAP Number
dN_T/dlogDa (cm^-3)
100
10
1
0.1
0.01
0.001
Mean
Median
25 - 75th Percent.
5 - 95th Percent.
5 6 7 8 9 1 2 3 4 5 6 7 8 9 10 2
Da (µm)

Figure S20.

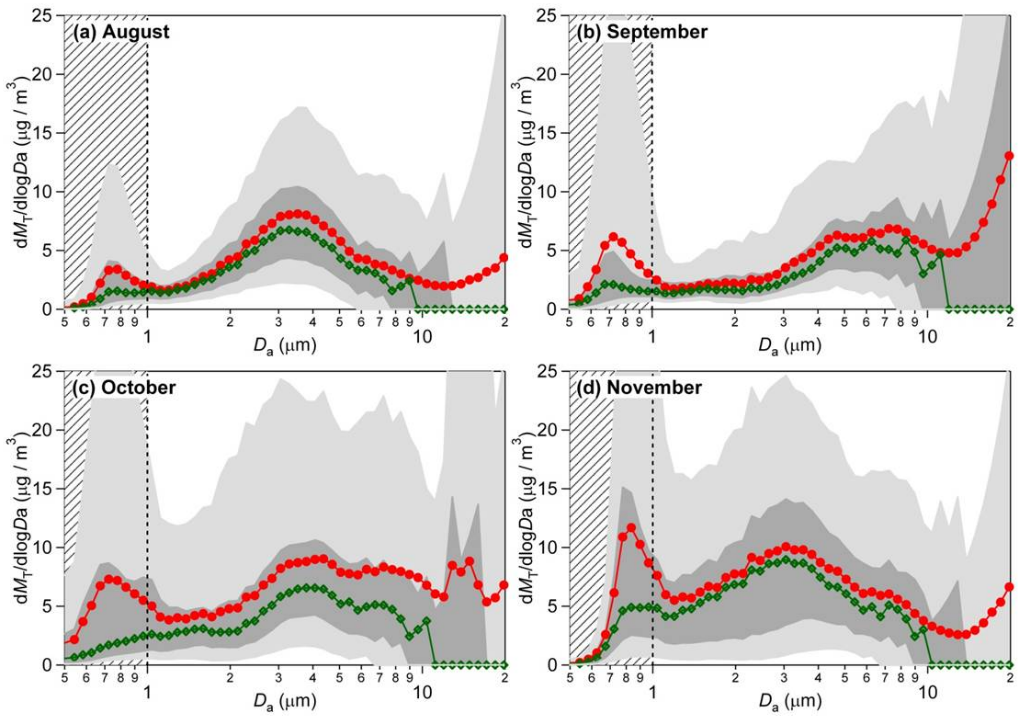
(a) August
(b) September
(c) October
(d) November
dMT/dlogDa (µg / m3)
Da (µm)
0
5
10
15
20
25
1
10

Figure S21.

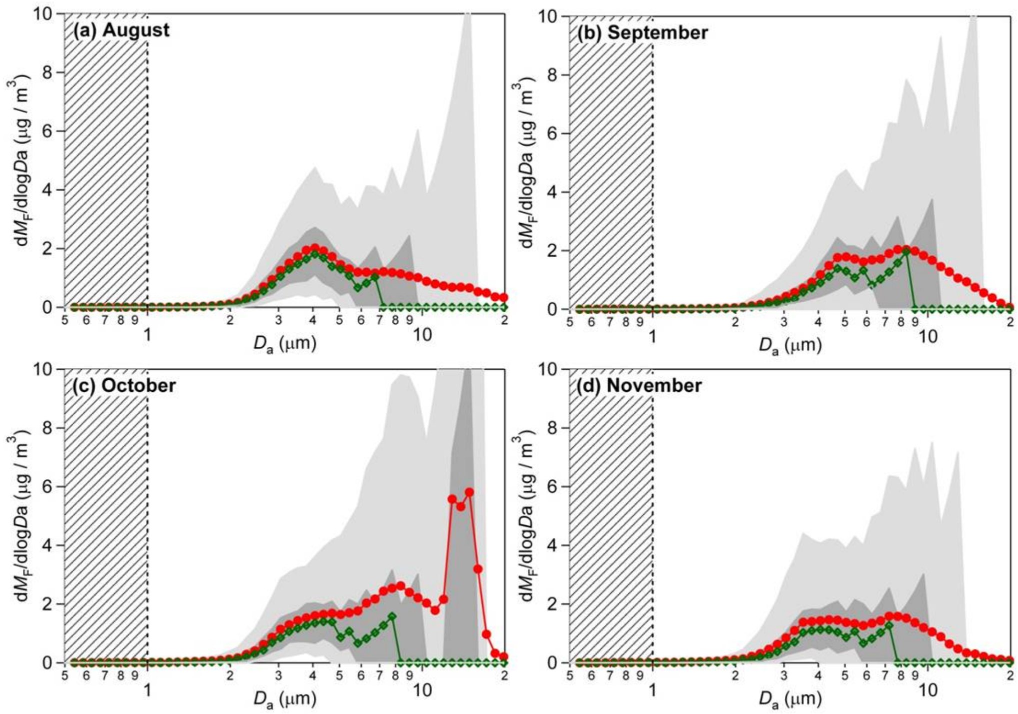
(a) August
(b) September
(c) October
(d) November
dM_F/dlogDa (µg / m^3)
D_a (µm)
0
2
4
6
8
10
5 6 7 8 9 1 2 3 4 5 6 7 8 9 10 2

Figure S22.

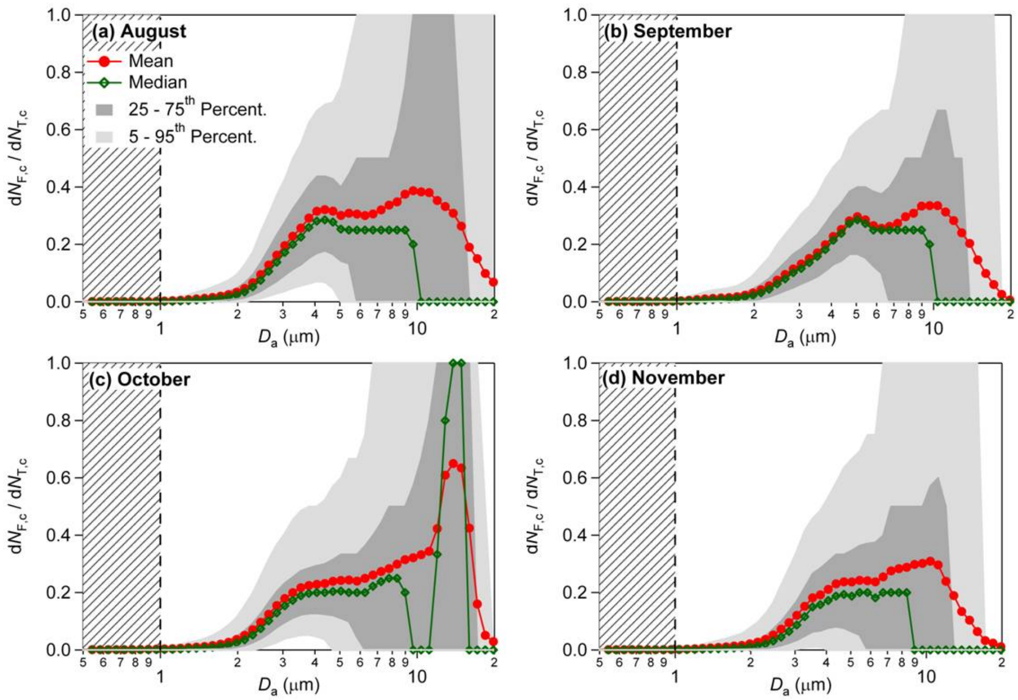
(a) August
Mean
Median
25 - 75th Percent.
5 - 95th Percent.
(b) September
(c) October
(d) November
dNF,c / dNT,c
Da (μm)
0.0
0.2
0.4
0.6
0.8
1.0
5 6 7 8 9 1 2 3 4 5 6 7 8 9 10 2

Figure S23.

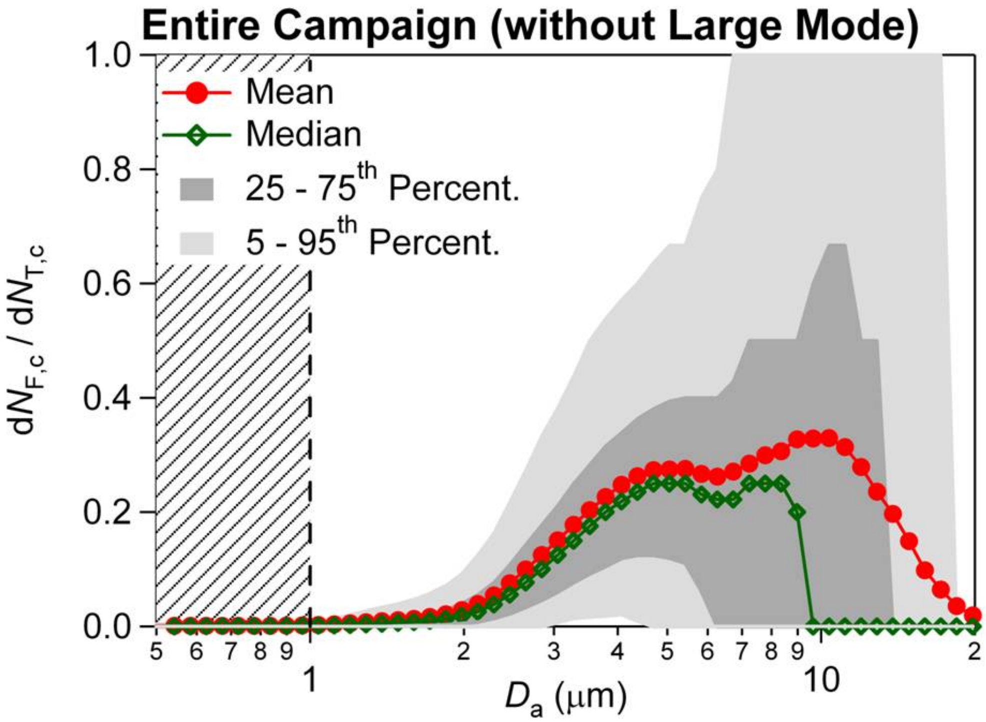
Entire Campaign (without Large Mode)
Mean
Median
25 - 75th Percent.
5 - 95th Percent.
dNF,c / dNT,c
1.0
0.8
0.6
0.4
0.2
0.0
5 6 7 8 9
1
2
3
4
5 6 7 8 9
10
2
Da (µm)

Figure S24.